10.48047/jocaaa.2026.35.06.18

A Hybrid Finite Difference and RBF-FD Simulation of Flow over a NACA 0012 Airfoil at Multiple Angles of Attack

Nikunja Bihari Barik
PG Department of Mathematics, Government DAV College Koraput, Odisha, India
*Corresponding Email: nikunjamath@gmail.com

Abstract

An accurate hybrid mesh-based Finite Difference Method (FDM) and meshless Radial Basis Function-generated Finite Difference (RBF-FD) method is presented for in this paper. The method is developed for the simulation of two-dimensional incompressible potential flow over a NACA 0012 airfoil. The classical FDM is employed in the structured far-field region to ensure computational efficiency, while the RBF-FD local correction is applied near the airfoil surface to improve numerical accuracy in regions with strong geometric curvature for multiple angles of attack (AoA).

Keywords: Meshfree method, NACA 0012 airfoil problem, angles of attack, Streamline.

AMS Subject classifications: 65Y04; 65Y15; 35Q35

1. INTRODUCTION

Accurate numerical simulation of aerodynamic flow around airfoils remains a fundamental topic in computational fluid dynamics due to its importance in aerospace and spacecraft engineering, mechanical engineering, automotive aerodynamics and renewable energy applications. Airfoils are streamlined aerodynamic shapes designed to generate lift when moving through a fluid such as air. They are fundamental components in a wide range of engineering systems including aircraft wings, helicopter propellers, racing vehicles, wind turbine blades, and unmanned aerial vehicles (UAVs). The aerodynamic performance of an airfoil plays a crucial role in determining lift production, drag minimization, flow stability, and the overall energy efficiency of aerodynamic systems [1,2]. Numerical methods are essential for solving the governing equations around complex geometries such as airfoils. Among classical approaches, the Finite Difference Method (FDM) is one of the simplest and most efficient techniques for solving partial differential equations on structured grids. FDM provides reliable global solutions with strong stability and convergence characteristics, making it one of the most widely used numerical techniques for solving partial differential equations in computational fluid dynamics [3, 4]. However, when dealing with curved geometries such as airfoil surfaces, conventional Cartesian FDM grids often experience geometric inaccuracies and inadequate local resolution near the boundary. In contrast, mesh-free methods are highly effective for handling complex geometries. A key advantage of mesh-free approaches is that they eliminate the need for mesh generation, which is typically a time-consuming task for complicated computational domains [5, 6]. Since meshfree methods employ arbitrarily distributed nodal points to discretize the domain, the computational cost associated with mesh generation is significantly reduced [7, 8]. Consequently, research on meshfree methods has attracted considerable attention in both mathematics and interdisciplinary engineering applications. The integration of FDM and RBF-FD provides an efficient hybrid numerical framework for aerodynamic flow simulation. In this approach, the FDM is utilized to evaluate the global flow field on a structured Cartesian grid, whereas the RBF-FD technique is

10.48047/jocaaa.2026.35.06.18

applied locally near the airfoil boundary to enhance numerical accuracy. This hybrid strategy combines the computational efficiency and simplicity of FDM with the superior boundary representation capability of meshfree RBF methods.

In the present study, a hybrid FDM and RBF-FD solver is developed to simulate flow around a NACA 0012 airfoil. The two-dimensional Laplace equation governing the velocity potential is solved over the computational domain for various angles of attack. Numerical results are presented in terms of velocity magnitude contours, pressure distributions, and streamline patterns. The investigation highlights the capability of integrating structured-grid finite difference techniques with local meshfree corrections to achieve improved accuracy in aerodynamic flow simulations.

2. Mathematical Formulation and Airfoil Geometry

Consider a two-dimensional, incompressible, inviscid, and irrotational flow over a symmetric NACA 0012 airfoil. The fluid density remains constant and viscous shear stresses are neglected. Since the flow is irrotational, the vorticity vanishes, i.e.,

$$\boldsymbol{\nabla x V} = \mathbf{0}$$

where $\boldsymbol{V} = (\boldsymbol{u}, \boldsymbol{v})$ denotes the velocity vector in Cartesian coordinates.

For irrotational flow, the velocity field can be represented by a scalar velocity potential $\Phi(x, y)$ such that $\boldsymbol{V} = \boldsymbol{\nabla}\,\Phi,$ or equivalently $u = \frac{\partial \Phi}{\partial x}, v = \frac{\partial \Phi}{\partial y}$

Because the fluid is incompressible, the continuity equation is $\boldsymbol{\nabla . V} = \mathbf{0}$

Substituting $\boldsymbol{V} = \boldsymbol{\nabla}\,\Phi$ into the continuity equation gives $\boldsymbol{\nabla}\,.\,(\boldsymbol{\nabla}\Phi) = 0$

Hence, the governing equation for the velocity potential becomes Laplace's equation. This elliptic partial differential equation is solved numerically in the computational domain surrounding the airfoil.

Boundary Conditions

1. On the airfoil surface, the no-penetration condition is imposed. $\frac{\partial \Phi}{\partial n} = 0$, where n denotes the outward normal direction.
2. At the far-field boundary, the uniform free-stream condition is applied. $\Phi = U_\infty(x \cos\alpha + y\, sin\,\alpha)$, where U_∞ is the free-stream velocity and α is the angle of attack.

Airfoil Geometry

For the NACA 0012 airfoil, the thickness distribution is

$y_t = 5t(0.2969\,\sqrt{\mathrm{x}} - 0.1260\,\mathrm{x} - 0.3516\,\mathrm{x}^2 + 0.2843x^3 - 0.1015x^4)$,

where $t = 0.12$. The upper and lower surfaces are defined as $y_u = +y_t, y_l = -y_t$. NACA \$0012\$ airfoil geometry presented in the Figure 1.

10.48047/jocaaa.2026.35.06.18

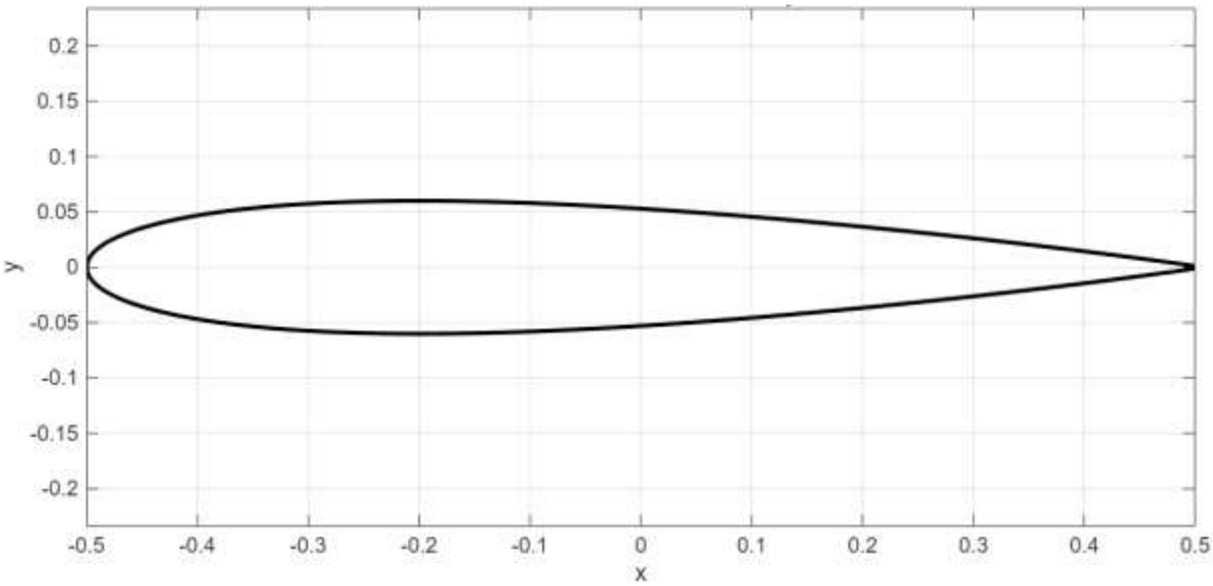

Figure 1: NACA 0012 Airfoil Geometry

3. Mathematical Methodology

First Laplace equation is solved using FDM. Then the solution near the NACA 0012 airfoil boundary is refined by RBF-FD method. Thus, the hybrid FDM + RBF-FD method combines the efficiency of structured-grid solvers with the advantage of geometric flexibility in meshfree methods.

3.1 Finite Difference Approximation

The central finite differences formula used to approximate the second derivatives.

$$\frac{\partial^2 \Phi}{\partial^2 x} \approx \frac{\Phi_{i+1,j} - 2\Phi_{i,j} + \Phi_{i-1,j}}{\Delta x^2},$$

$$\frac{\partial^2 \Phi}{\partial^2 y} \approx \frac{\Phi_{i,j+1} - 2\Phi_{i,j} + \Phi_{i,j-1}}{\Delta y^2}$$

By using in Laplace equation gives

$$\frac{\Phi_{i+1,j} - 2\Phi_{i,j} + \Phi_{i-1,j}}{\Delta x^2} + \frac{\Phi_{i,j+1} - 2\Phi_{i,j} + \Phi_{i,j-1}}{\Delta y^2} = 0$$

For $\Delta x = \Delta y, \Phi_{i,j} = 0.25(\Phi_{i+1,j} + \Phi_{i-1,j} + \Phi_{i,j+1} + \Phi_{i,j-1})$

The Gauss-Seidel method is used to solve the algebraic system of the discretized equations. The maximum absolute residual error (Error=max $|\Phi^{(k+1)} - \Phi^{(k)}|$) is calculated with error tolerance less than 10^{-6} to get the convergence. The velocity components are obtained using first-order central differences.

10.48047/jocaaa.2026.35.06.18

3.2 RBF-FD Formulation

The RBF interpolation is defined by

$$\Phi(x) \approx \sum_{i=1}^{m} \lambda_i \psi(||x - x_i||) + \sum_{j=1}^{n} \beta_j P_j(x), x \epsilon \mathbb{R}^d \quad (1)$$

where $||x - x_i||$ is the Euclidean norm of the difference between x and x_i, $P_j(x), j = 1,2, \dots N$ is a basis for $\Pi_n(\mathbb{R}^d)$. λ_i and β_j can be determined by solving the following symmetric linear system.

$$\left(\begin{array}{c|c} C & P \\ \hline P^T & 0 \end{array}\right)\left(\begin{array}{c} \lambda \\ \hline \beta \end{array}\right) = \left(\begin{array}{c} G \\ \hline 0 \end{array}\right) \quad (2)$$

where $C = [c_{ki}]_{nxn} = \left[\psi\left(||x_i - x_k||\right)\right]_{nxn}$ and $P = [P_j(x_i)]_{mxN}$, $i = 1,2, \dots n, k = 1,2, \dots, N, j = 1,2, \dots, N$. In the present work, the Gaussian radial basis function $\psi = e^{-(\varepsilon r)^2}$ is employed, where $r_k = \sqrt{(\mathrm{x} - \mathrm{x_k})^2 + (\mathrm{y} - \mathrm{y_k})^2}$, ε is the shape parameter controlling smoothness. The RBF-FD correction is applied only near the airfoil surface. For each fluid

$d_{min} = \min_k \left[\left(x - x_{\alpha,k}\right)^2 + \left(y - y_{\alpha,k}\right)^2\right]$. If $d_{min} < \delta$ where δ is a prescribed threshold distance, then RBF correction is activated for the nodes.

4. Results and Discussion

The hybrid numerical model based on the FDM and RBF-FD was employed to simulate inviscid incompressible flow over the NACA 0012 airfoil for angles of attack $\alpha = -10^o, -5^o, 0^o, 5^o, 10^o, 15^o$. The velocity magnitude is calculated from $V = \sqrt{\mathrm{u}^2 + \mathrm{v}^2}$ with $u = \frac{\partial \Phi}{\partial x}, v = \frac{\partial \Phi}{\partial y}$. The velocity magnitude with different AoA are plotted and presented in Figure 2. It confirms that nearly equal velocity on both surfaces for 0^o AoA. So it is zero lift for symmetric case. At $\alpha = 10^o$ and 15^o, a concentrated high-speed region appears near the upper leading edge. This corresponds to a strong suction peak and increasing lift. For negative angles, the high-speed zone shifts to the lower surface. This indicates decreasing of lift. The result is matching theoretical expectations from thin airfoil theory [9, 10]. The pressure field was computed using Bernoulli relation, $P = P_\infty + 0.5\rho(U_\infty^2 - V^2)$. The Pressure field with different AoA are plotted and presented in Figure 3. At zero incidence, the pressure contours are nearly symmetric. A stagnation pressure maximum appears near the nose of the airfoil where velocity approaches zero. For positive incidence, the upper surface develops a large low-pressure zone, especially near the leading edge. Simultaneously, the lower surface pressure becomes comparatively higher. This pressure difference generates upward lift. It is observed that the pressure field obtained using the proposed methods shows good agreement with the theoretical airfoil results [11, 12]. The streamlines illustrate the instantaneous direction of flow around the airfoil. The streamlines with different AoA are plotted and presented in Figure 4. At $\alpha = 0^o$ streamlines split symmetrically at the nose and

10.48047/jocaaa.2026.35.06.18

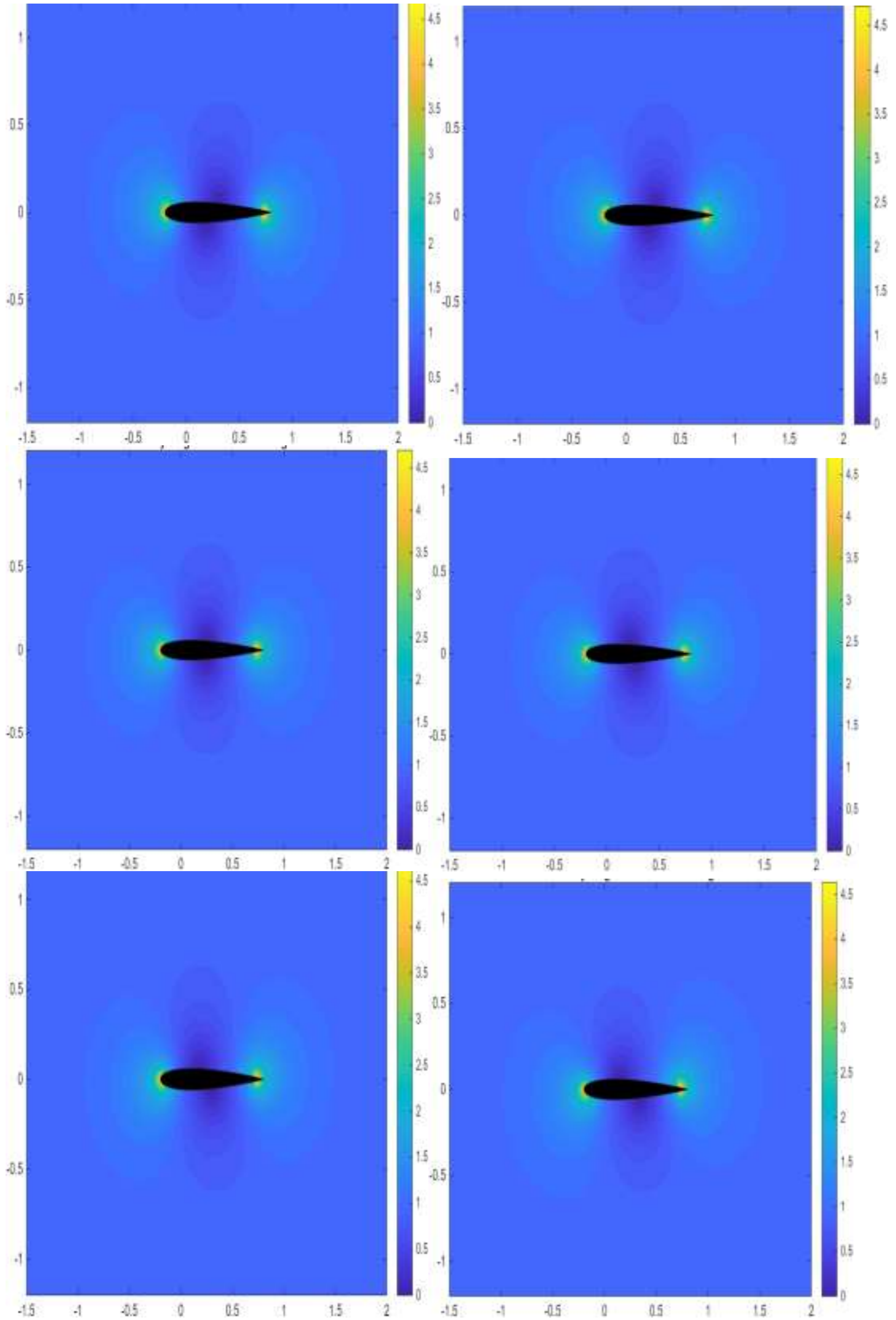

Figure 2: Velocity Magnitude with AoA $-10^{o}, -5^{o}, 0^{o},\ 5^{o}, 10^{o}, 15^{o}$(from top left to right)

10.48047/jocaaa.2026.35.06.18

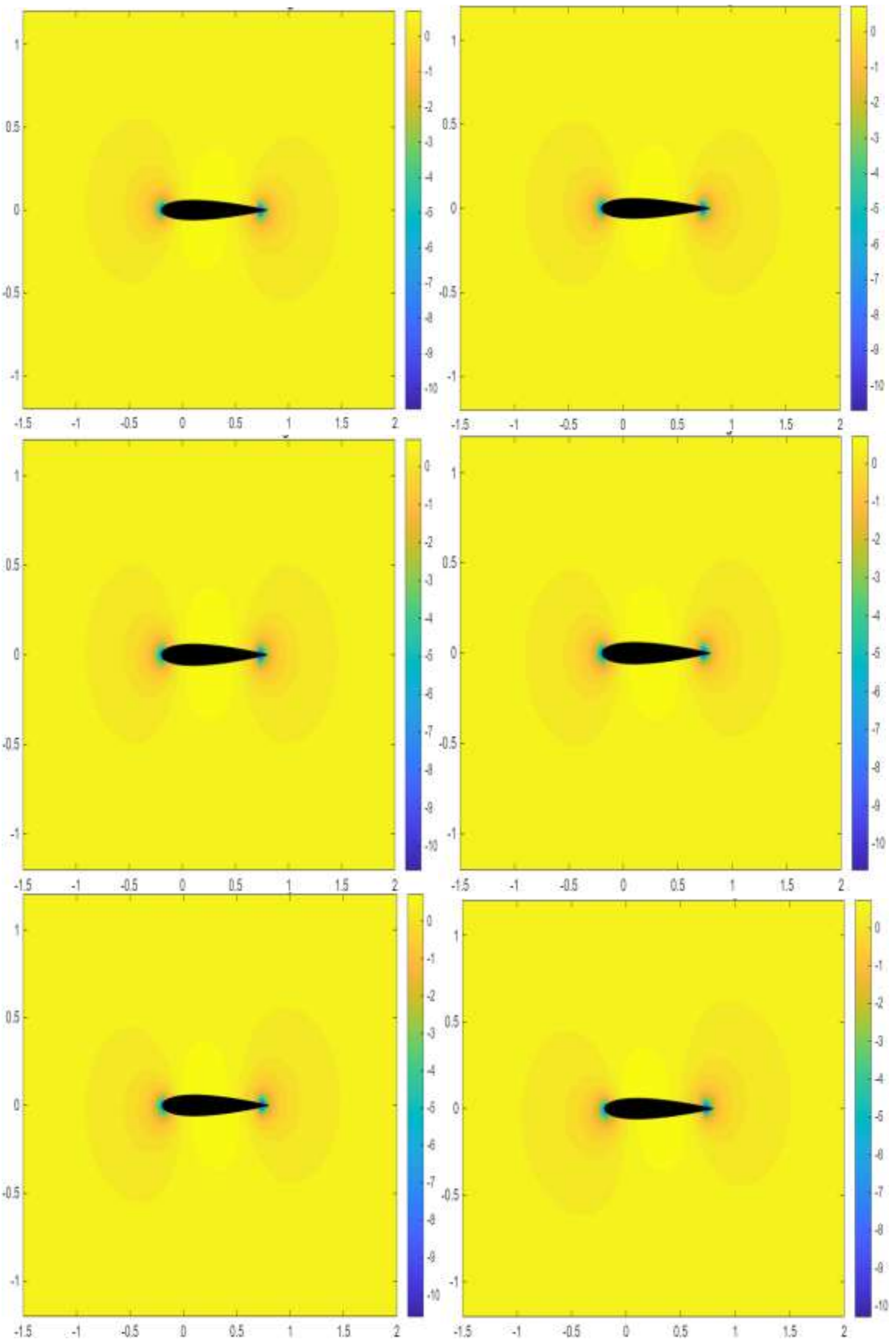

Figure 3: Pressure Contour with AoA $-10^o, -5^o, 0^o,\ 5^o, 10^o, 15^o$(from top left to right)

10.48047/jocaaa.2026.35.06.18

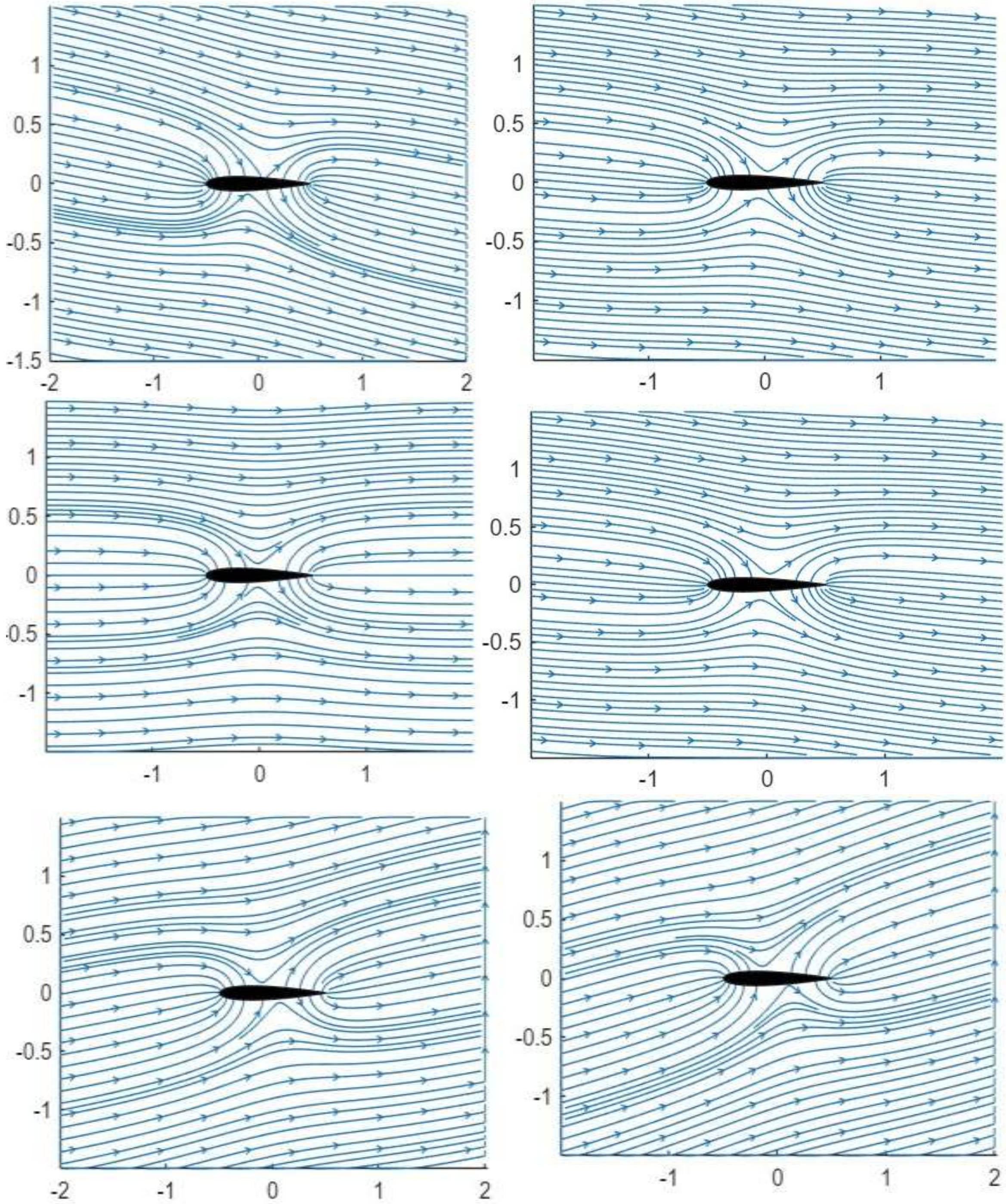

Figure 4: Streamline with AoA $-10^o, -5^o, 0^o,\ 5^o, 10^o, 15^o$(from top left to right)

reunite at the trailing edge. For positive incidence, streamlines bend upward over the top surface and downward below the body. At larger positive angles, streamline curvature becomes stronger, especially near the leading edge. This indicates stronger aerodynamic loading. For negative incidence, the streamline deflection reverses direction, producing downward aerodynamic force. This behavior agrees with classical aerodynamic flow visualization around lifting bodies [11].

10.48047/jocaaa.2026.35.06.18

5. Conclusions

This paper presented a hybrid mesh-based and meshless numerical framework combining the FDM and RBF-FD method is developed for NACA 0012 airfoil over a wide range of incidence angles. The classical FDM solved the governing equation efficiently while RBF-FD correction improved solution smoothness near curved boundaries. The predicted velocity magnitude, pressure contour and streamline curvature are all physically consistent with classical airfoil theory.

Acknowledgement

Author thank Odisha State Higher Education Council (OSHEC), Department of Higher Education, Government of Odisha for financial support provided under MRIP-2023 funding with reference no. 23EM/MT/98.

Conflicts of interest

No Animals are involved in the research work.

Funding

This work was financially supported by the OSHEC, Department of Higher Education, Government of Odisha.

References

[1] Hirsch, C., *Numerical Computation of Internal and External Flows,* Computers \& Fluids, 17(1989), pp. 385–386.

[2] P. R. Spalart and S. R. Allmaras, *A One-Equation Turbulence Model for Aerodynamic Flows,* AIAA Journal, 94 (1994).

[3] H. J. Schroll, *Convergence of implicit finite difference methods applied to nonlinear mixed systems*, SIAM journal on numerical analysis, 33 (1996), pp. 997--1013.

[4] Guan, Tianen and Huang, Zijia and Xu, Chunguang, *Theoretical and Computational Fluid Dynamics,* 39 (2025), pp. 26.

[5] B. Fornberg, and N. Flyer, A Primer on Radial Basis Functions with Applications to the Geosciences, *Society for Industrial and Applied Mathematics, Philadelphia,* 2015.

[6] G. B. Wright, and B. Fornberg, Scattered node compact finite difference-type formulas

10.48047/jocaaa.2026.35.06.18

generated from radial basis functions, *J. Comput. Phys.,* vol. 212, no. 1, pp. 99--123, February 2006.

[7] N. B. Barik, and T. V. S. Sekhar, A novel RBF-FD meshless scheme in curvilinear geometry for unbounded flows, *Int. J. Comput. Methods Eng. Sci. Mech.,* vol. 18, no. 4-5, pp. 209--219, June 2017.

[8] N. B. Barik, and T. V. S. Sekhar, An efficient local RBF meshless scheme for steady convection-diffusion problems, *Int. J. Comp. Meth.,* vol. 14, no. 6, pp. 1750064, January 2017.

[9] J. D. Anderson, *Fundamentals of Aerodynamics*, 5th ed., McGraw-Hill, 2010.

[10] J. Katz and A. Plotkin, *Low-Speed Aerodynamics*, Cambridge University Press, 2001.

[11] F. M. White, *Fluid Mechanics*, 7th ed., McGraw-Hill, 2011.

[12] I. H. Abbott and A. E. Von Doenhoff, *Theory of Wing Sections*, Dover Publications, 1959.